

1 **Choice of host cell line is essential for the functional glycosylation of**
2 **the fragment crystallizable (Fc) region of human IgG1 inhibitors of**
3 **influenza B viruses**

4
5 Patricia A. Blundell[§], Dongli Lu*, Anne Dell*, Stuart M. Haslam* and Richard
6 J. Pleass^{§1}

7
8 From the [§]Department of Tropical Disease Biology, Liverpool School of
9 Tropical Medicine, Liverpool, L3 5QA, United Kingdom.

10
11 *Department of Life Sciences, Imperial College London, London, SW7 2AZ,
12 United Kingdom.

13
14
15 **Running title:** Cell line dependent differences in functional Fc-glycosylation

16
17 **Key words:** IgG, immunoglobulin, Fc-receptors, lectin, glycan, sialic acid,
18 sialylation, siglec, C-type lectin, Fc-multimers, Fc-monomers, IVIG,
19 complement, influenza virus, agglutination

20
21
22 ¹. To whom correspondence should be addressed: Dept. of Parasitology,
23 Liverpool School of Tropical Medicine, Pembroke Place, Liverpool, L3 5QA,
24 United Kingdom. Tel: 44-151-345-7793; e-mail: richard.pleass@lstm.ac.uk

25
26 ². The abbreviations used are: Fc, Fragment crystallizable; IVIG, Intravenous
27 Immunoglobulin; ITP, Idiopathic Thrombocytopenic Purpura; tp, tailpiece;
28 Siglec, Sialic acid-binding immunoglobulin-type lectin; CD, Cluster
29 Designation; CHO, Chinese Hamster Ovary; DC-SIGN, Dendritic Cell-Specific
30 Intercellular Adhesion Molecule-3-grabbing Non-Integrin; DCIR, C-type Lectin
31 Dendritic Cell Immunoreceptor; CLEC, C-type Lectin; HA, Hemagglutinin; HIA,
32 Hemagglutination Inhibition Assay; HEK 293-F, Human Endothelial Kidney;
33 MBL, Mannose-Binding Lectin; MMR, Macrophage Mannose Receptor; mAbs,
34 monoclonal Antibody; MALDI, matrix-assisted laser desorption ionisation;
35 TOF, time-of-flight; SE-HPLC, Size Exclusion-High Performance Liquid
36 Chromatography.

37
38 This work was supported by Pathfinder and Innovator grants from the
39 Wellcome Trust (109469/Z/15/Z and 208938/Z/17/Z) and Institutional
40 Strategic Support Fund (ISSF) 109469/Z/15/Z, 208938/Z/17/Z, 097830/Z/11/Z
41 from the Wellcome Trust and MRC Confidence in Concept award
42 MC_PC_12017 respectively. Also, by the Biotechnology and Biological
43 Sciences Research Council grant BBF0083091 (A. Dell and S.M. Haslam).

51 **Abstract**

52 **Antibodies are glycoproteins that carry a conserved N-linked carbohydrate**
53 **attached to the Fc, whose presence and fine structure profoundly impacts on**
54 **their *in vivo* immunogenicity, pharmacokinetics and functional attributes. The**
55 **host cell line used to produce IgG has a major impact on this glycosylation, as**
56 **different systems express different glycosylation enzymes and transporters**
57 **that contribute to the specificity and heterogeneity of the final IgG-Fc**
58 **glycosylation profile. Here we compare two panels of glycan-adapted IgG1-Fc**
59 **mutants expressed in either the HEK 293-F or CHO-K1 systems. We show that**
60 **the types of N-linked glycans between matched pairs of Fc mutants vary**
61 **significantly, and in particular with respect to sialylation. These cell line effects**
62 **on glycosylation profoundly influence the ability of the engineered Fcs to**
63 **interact with either human or pathogen receptors. For example, we describe Fc**
64 **mutants that potently disrupted influenza B-mediated agglutination of human**
65 **erythrocytes when expressed in CHO-K1 but not in HEK 293-F cells.**

66

67

68

69

70

71

72

73

74

75

76

77

78

79

80

81

82

83

84

85

86

87

88

89

90

91

92

93 Introduction

94 In therapeutic approaches where the Fc of human IgG1 is critically important,
95 receptor binding and functional properties of the Fc are lost after de-
96 glycosylation or removal of the Asn-297 N-linked glycosylation attachment site
97 located in the body of the Fc (1–3). More detailed studies into the types of
98 sugars involved in this functionality have shown enhanced Fc γ RIIIA binding
99 and ADCC of IgG1 in the absence of fucose (4, 5); enhanced Fc γ RIIIA binding
100 but rapid clearance from the circulation of IgG1 enriched for oligomannose
101 structures (6–8); improved solubility, anti-inflammatory activity, thermal
102 stability and circulatory half-life of terminally sialylated glycans from IgG1 (9–
103 13).

104 These findings have generated an incentive to modify the existing IgG1
105 glycans attached to Asn-297, either by chemical means (12, 14), by
106 mutagenesis programs on the Fc protein backbone that disrupt the protein-
107 Asn-297-carbohydrate interface (15), or by expression in glycosidase-adapted
108 transgenic cell lines (reviewed in 16). For example, the FDA approved
109 humanized antibody Mogamulizumab, which is used to treat lymphoma and is
110 manufactured in CHO cell lines in which the α (1-6)-fucosyltransferase (*FUT8*)
111 gene is removed, results in an afucosylated IgG1 with enhanced Fc γ RIIIA-
112 dependent tumour cell killing by ADCC (17). Although similar approaches
113 have yielded enhanced sialylation of IgG, with zero to moderate
114 improvements in binding to Fc γ Rs (12, 15, 18, 19), these have not led to
115 significant enhancements in binding to inhibitory glycan receptors that are
116 important in controlling unwanted inflammation (19, 20), a finding we and
117 others have attributed to the buried location of the Asn-297 attached glycan
118 within the Fc (21, 22).

119 We took an alternative approach to enhancing the sialic acid content of
120 the Fc of IgG1 (23, 24), by adding the 18 amino-acid tailpiece (tp) from IgM to
121 the C-terminus of the IgG1 Fc, into which a cysteine-to-alanine substitution is
122 made at Cys-575, and including an extra N-glycosylation site to the N-
123 terminus at position Asn-221. The tp also contains a N-glycosylation site at
124 Asn-563. When expressed in CHO-K1 cells, these molecules displayed
125 enhanced binding to the low-affinity Fc γ -receptors (Fc γ RIIIA and Fc γ RIIB), and

126 to multiple glycan receptors that control excessive inflammation by IVIG (23–
127 25). Two such hyper-sialylated molecules (D221N/C575A and
128 D221N/C309L/N297A/C575A) also bound recombinant hemagglutinin from
129 influenza A and B viruses, and disrupted influenza A-mediated agglutination
130 of human erythrocytes (24).

131 Chinese hamster ovary (CHO) cell-based systems remain by far the
132 most common mammalian cell line used by the pharmaceutical industry; 84%
133 of products are produced in this cell system, and the remaining approved
134 antibodies are produced in either NS0 or Sp2/0 cells (26). Although CHO cells
135 account for the largest number of FDA approved bio-therapeutics (26), they
136 do not express α 1,2/3/4 fucosyltransferase and β -1-4-N-acetylglucosaminyl-
137 transferase III, which are enzymes expressed in human cells (27).
138 Furthermore, humans have active α 2,6-sialyltransferase. As such, CHO
139 derived IgG1 Fcs are only sialylated through α 2,3 linkages whereas both α 2,3
140 and α 2,6 linkages can be found on human IgG1 Fc (23, 27). Most non-human
141 mammalian cell lines can also attach Neu5Gc. Humans do not have an active
142 CMP-Neu5Ac hydroxylase so do not attach Neu5Gc, which can elicit
143 immunogenic responses (27) and consequently non-human cell lines are
144 stringently screened to identify clones that produce proteins with desirable
145 glycan profiles (28).

146 Human cell lines are a promising alternative to non-human cell lines as
147 they possess fully human post-translational modifications that reduce
148 downstream processing costs and, more importantly, circumvent any risks
149 associated with immunogenicity from non-human glycans. However, human
150 cell lines also have significant limitations, including the capacity to produce
151 sialyl-Lewis^x which binds to endothelial selectins in areas of inflammation (29).
152 Although this may potentially be favourable for anti-inflammatory therapies
153 (29), the attached sialyl-Lewis^x may also adversely affect the biodistribution
154 and pharmacokinetics of a Fc when used in other clinical contexts, for
155 example anti-tumor mAbs. Human cell lines also carry the risk of
156 contamination and forward transmission of human pathogens, in particular
157 viruses, that may explain why CHO-K1 cells are still the preferred cell line
158 used by the pharmaceutical industry. These issues led us to compare the

159 functional properties of a panel of Fc mutants generated in CHO-K1 cells with
160 the same set of proteins manufactured by HEK 293-F cells (24).

161

162

163

164

165

166

167

168

169

170

171

172

173

174

175

176

177

178

179

180

181

182

183

184

185

186

187

188

189

190

191

192

193 **Materials and Methods**

194 *Production of mutants*

195 The generation of glycan mutants in all combinations has been described
196 previously for the hexa-Fc that contains cysteines at both positions 309 and
197 575 (23). To make the new mutants described in Fig. 1 in which Cys-575 was
198 mutated to alanine, PCR overlap extension mutagenesis was used with a pair
199 of internal mismatched primers 5'-ACCCTGCTTGCTCAACTCT-3' / 3'-
200 GGCCAGCTAGCTCAGTAGGCGGTGCCAGC-5' for each plasmid vector
201 coding for a designated glycan modification. The parental plasmids used for
202 these new PCR reactions have been described previously (23). The resulting
203 C575A mutants were then further modified to remove Cys-309 using primer
204 pair 5'-TCACCGTCTTGCACCAGGACT-3' / 3'-
205 AGTCCTGGTGCAAGACGGTGA-5' to create the panel of double cysteine
206 knockouts described in Fig. 2. To verify incorporation of the desired mutation
207 and to check for PCR-induced errors, the open reading frames of the new
208 mutants were sequenced on both strands using previously described flanking
209 primers (23). CHO-K1 cells (European Collection of Cell Cultures) were stably
210 transfected with plasmids using FuGene (Promega), stable cell lines were
211 created, and Fc-secreting clones were expanded and proteins purified as
212 previously described (30, 31). HEK 293-F cells were transiently transfected
213 using the FreeStyle MAX293 expression system (Life Technologies) and
214 proteins purified as for CHO-K1 cells.

215

216 *Size analysis using SE-HPLC*

217 A SEC3000 [300 x 7.8 mm] column (Beckman) was set up on a Dionex
218 ICS3000 HPLC system and pre-equilibrated with 0.2 µm filtered PBS. Protein
219 samples at concentrations ranging from 0.5-1 mg/mL were placed in a pre-
220 cooled auto-sampler at 4°C and 10 µL of each was sequentially injected onto
221 the column. Each sample was run for 1.5 column volumes in PBS at a flow
222 rate of 0.25 mL/min. Elution was monitored at 280 and 214 nm. The column
223 was calibrated by running standard proteins (BioRad: thyroglobulin, bovine
224 IgG, ovalbumin, myoglobin and cyanocobalamin) under the same conditions.

225 *Receptor and complement binding assays*

226 Methods describing the binding of mutants to tetrameric human DC-SIGN
227 (Elicityl), Siglec-1, Siglec-4, and Siglec-3 (Stratech Scientific) have all been
228 described previously (30, 31). The same ELISA protocol was used for Siglec-
229 2, CD23, dec-1, dec-2, clec-4a, clec-4d, MBL and MMR (Stratech Scientific or
230 Bio-Techne). Binding of C1q has been described previously (30, 31). ELISAs
231 were used to investigate binding of Fc glycan mutants to human Fc γ RI,
232 Fc γ RIIA, Fc γ RIIB, Fc γ RIIIA, and Fc γ RIIIB (Bio-Techne). Receptors were
233 coated down onto ELISA plates (Nunc) in carbonate buffer pH 9 (Sigma-
234 Aldrich) at 2 μ g/ml overnight at 4°C, unless otherwise specified. The plates
235 were blocked in PBS / 0.1% Tween-20 (PBST) containing 5% dried skimmed
236 milk. Plates were washed three times in PBST before adding Fc mutant
237 proteins at the indicated concentrations and left at 4°C overnight. Plates were
238 washed as above and incubated for 2h with 1:500 dilution of an alkaline
239 phosphatase-conjugated goat F(ab')₂ anti-human IgG (Jackson Laboratories).
240 Plates were washed and developed for 15 min with 100 μ l/well of a Sigmafast
241 *p*-nitrophenyl phosphate solution (Sigma-Aldrich). Plates were read at 405nm,
242 and data plotted with GraphPad Prism.

243

244 *Hemagglutination inhibition assay (HIA)*

245 Native influenza B Hong-Kong 5/72 was obtained from Meridian Life
246 Sciences. To determine the optimal virus-to-erythrocyte ratio, two-fold virus
247 stock dilutions were prepared in U-shaped 96-well plates (Thermo Scientific).
248 The same volume of a 1% human O+ red blood cell suspension (Innovative
249 Research) was added to each well and incubated at room temperature for 1h
250 until erythrocyte pellets had formed. After quantifying the optimal virus-to-
251 erythrocyte concentration (4HA units), serial two-fold dilutions of Fc, control
252 IVIG (GammaGard, Baxter Healthcare) and polyclonal goat anti-influenza B
253 (Biorad) were prepared, all starting at a concentration of 2 μ M, and mixed with
254 50 μ l of the optimal virus dilution. After 30 min incubation at room
255 temperature, 50 μ l of the human erythrocyte suspension was added to all
256 wells, and plates incubated at room temperature for 1h, after which

257 erythrocyte pellets could be observed in the positive controls and positive
258 samples.

259

260 *Binding to Fc γ Rs by Biacore*

261 Binding to Fc γ Rs was carried out using a Biacore T200 biosensor (GE
262 Healthcare). Recombinantly expressed Fc γ RS (R&D systems or Sino
263 Biologicals) were captured via their histidine tags onto CM5 chips pre-coupled
264 with ~9000 reflective units anti-His Ab (GE Healthcare) using standard amine
265 chemistry. Fc mutants were injected over captured receptors at a flow rate of
266 20 μ l/min, and association and dissociation monitored over indicated time
267 scales before regeneration with two injections of glycine (pH 1.5) and
268 recalibration of the sensor surface with running buffer (10 mM HEPES, 150
269 mM NaCl [pH 7]). Assays were visualized with Biacore T200 evaluation
270 software v2.0.1.

271

272 *N-glycomic analysis*

273 N-glycomic analysis was based on previous developed protocol with some
274 modifications (32). Briefly, the N-glycans from 50 μ g of each sample were
275 released by incubation with NEB Rapid™ PNGase F and isolated from
276 peptides using Sep-Pak C18 cartridges (Waters). The released N-glycans
277 were permethylated, prior to Matrix-assisted laser desorption ionization
278 (MALDI) MS analysis. Data were acquired using a 4800 MALDI-TOF/TOF
279 mass spectrometer (Applied Biosystems) in the positive ion mode. The data
280 were analyzed using Data Explorer (Applied Biosystems) and
281 Glycoworkbench (33). The proposed assignments for the selected peaks were
282 based on composition together with knowledge of biosynthetic pathways.

283

284

285

286

287

288

289

290 **Results**

291

292 ***Disulfide bonding and glycosylation influence the multimerization states***
293 ***of Fc mutants expressed by HEK 293-F cells***

294 Two panels of glycosylation- and cysteine-deficient mutants previously
295 expressed by CHO-K1 cells were generated in HEK 293-F cells (Figs. 1 and
296 2). As observed with CHO-K1 cells, the HEK 293-F cells were capable of
297 making all the mutants to high yields (~30 mg/L) with the exception of the
298 N297A/N563A/C575A mutant for which we were unable to generate sufficient
299 protein for further work. Generally, all the mutants migrated on SDS-PAGE
300 with the expected molecular weights for their glycosylation or disulfide
301 bonding states (Fig. 3), as previously described for the same mutants
302 expressed by CHO-K1 cells (23).

303 In an earlier study with CHO-K1 cells we demonstrated that a
304 proportion of molecules in which the tailpiece Asn-563 glycan was substituted
305 for alanine ran as multimers in solution when examined by SE-HPLC (24).
306 The loss of the bulky Asn-563 glycan exposes hydrophobic amino acid
307 residues in the tailpiece that facilitate non-covalent interactions in solution.
308 Such N563A-dependent multimerization was also observed with mutants
309 expressed by HEK 293-F cells, although the proportion of multimers to
310 monomers (with the notable exception of the N563A/C575A mutant) was
311 generally lower when mutants were made by this cell line (Fig. 4). Clearly, the
312 choice of cell line and consequently the types of post-translational
313 modifications, dramatically impact on the biophysical properties of these
314 molecules in solution.

315

316 ***Fc glycan mutants expressed by HEK 293-F cells show important***
317 ***differences in binding to glycan receptors when compared to CHO-K1***
318 ***proteins***

319 To determine the impact of the cell line on receptor binding by the two panels
320 of Fc mutants, we investigated their interaction with soluble recombinant
321 glycan receptors by ELISA (Fig. 5). For most of the Fc mutants, including
322 hexa-Fc, C575A, N297A/C575A, D221N/N297A/N563A/C575A,
323 C309L/C575A, D221N/C309L/C575A, D221N/C309L/N297A/C575A and

324 D221N/C309L/N297A/N563A/C575A, expression in HEK 293-F cells reduced
325 the binding to glycan receptors when compared to equivalent molecules
326 expressed in CHO-K1 cells (Fig. 5). However, two Fc mutants
327 (D221N/N563A/C575A and D221N/C309L/N573A/C575A) were notable for
328 their enhanced binding to all the glycan receptors investigated when
329 expressed in HEK 293-F cells. Given that both mutants multimerize poorly by
330 comparison to the equivalent mutants made in CHO-K1 cells (Fig. 4), we
331 attribute this enhanced glycan receptor binding not to increased avidity effects
332 but to fine differences in the attached glycan structures. Therefore, the choice
333 of cell line can dramatically impact on the ability of individual Fc mutants to
334 interact with glycan receptors.

335

336 ***Fc glycan mutants expressed by HEK 293-F cells show important***
337 ***differences in binding Fc γ -receptors compared to CHO-K1 cell proteins***

338 Given the observed differences in binding to glycan receptors of the same Fc
339 mutants expressed by two different cell lines, we also tested the impact of cell
340 line on binding to the classical human Fc γ Rs (Fig. 6).

341 The most significant difference observed was the ability of certain HEK
342 expressed mutants (N563A/C575A, D221N/N563A/C575A,
343 D221N/N297A/N563A/C575A, C309L/N563A/C575A,
344 C309L/N297A/N563A/C575A and D221N/C309L/N563A/C575A) to bind
345 human Fc γ RIIA (Arg-167) and Fc γ RIIIB. This is in stark contrast to the same
346 proteins expressed in CHO-K1 cells, where not one single mutant from each
347 panel bound either of the two low-affinity receptors (Fig. 6 and (24)).

348 To examine the interaction with human Fc γ RIIA (Arg-167) and Fc γ RIIIB
349 in more detail, we tested binding of two of these mutants
350 (C309L/N563A/C575A and D221N/C309L/N563A/C575A) to Fc γ RIIA (Arg-
351 167) and Fc γ RIIIB by surface plasmon resonance analysis (Fig. 7). Both
352 mutants displayed slower apparent off rates compared to the control IgG1-Fc
353 monomer, consistent with avidity effects either through binding to multiple
354 immobilized Fc γ R molecules or rebinding effects (Fig. 7). Therefore, the
355 choice of cell line impacts on the ability of individual Fc mutants to interact
356 with Fc γ Rs, and in particular Fc γ RIIA (Arg-167) and Fc γ RIIIB.

357

358 ***Fc glycan mutants expressed by HEK 293-F cells show improved***

359 ***binding to human C1q***

360 An important functional and safety attribute for therapeutic administration of
361 Fc fragments is their ability to bind C1q, and thus initiate the classical pathway
362 of complement activation. Binding of C1q was assessed by ELISA to selected
363 mutants expressed from each cell line (Fig. 8). Mutants D221N/C575A,
364 D221N/C309L/C575A, C309L/N297A/N563A/C575A and C309L/N563A/C575
365 expressed in HEK 293-F cells showed improved binding to C1q, compared to
366 their counterparts expressed in CHO-K1 cells, and no change in binding in
367 either direction was observed for IgG1-Fc, D221N/N563A/C575A,
368 D221N/N297A/C575A, D221N/C309L/N297A/C575A,
369 D221N/C309L/N297A/N563A/C575A, and C309L/N297A/C575A (Fig. 8).

370 Both the D221N/C575A and D221N/C309L/N297A/C575A mutants
371 from CHO-K1 cells have been shown previously to block influenza-mediated
372 hemagglutination (ref 23, and Fig. 11 below), and thus D221N/C575A
373 expressed in HEK 293-F cells that binds C1q may not be favored for clinical
374 development over the same molecule expressed by CHO-K1 cells (27).

375

376 ***Fc glycan mutants expressed in HEK 293-F cells have more complex***
377 ***glycosylation profiles than the equivalent mutants expressed in CHO-K1***
378 ***cells***

379 The structure of the N-glycan on the Fc of IgG antibodies has been shown to
380 influence multiple receptor interactions (3, 34, 35). Unlike the relatively simple
381 glycosylation of the Fc mutants previously described for CHO cells (23, 24),
382 HEK cells are capable of producing more complex N-glycan structures on
383 their glycoproteins (36).

384 We investigated the nature of the N-glycans on the two panels of
385 glycosylation- and cysteine-deficient mutants by MALDI-TOF mass
386 spectrometry-based glycomic analysis (complete data set for both panels of
387 mutants provided in supplementary figures). A core-fucosylated biantennary
388 structure without antennary galactosylation, m/z 1835 (GlcNAc₄Man₃Fuc₁), is
389 the base peak of spectra from all IgG1-Fc mutants produced by HEK cells
390 (Fig. 9 and supplementary figures).

391 The types of site-specific glycans attached to either Asn-221, Asn-297
392 or Asn-563 could be determined using both the C575A or C309L/C575A
393 panels of mutants. For example, only sugars attached to Asn-297 are
394 available for sampling in either the N563A/C575A or C309L/N563A/C575A,
395 mutants that therefore also allow the contribution of disulfide bonding to
396 glycosylation at Asn-297 to be elucidated.

397 The N-glycosylation of Asn-297 is dominated by core-fucosylated bi-
398 antennary glycans (m/z 1835 and 2040) with varied galactosylation levels
399 ($\text{Gal}_{0-2}\text{GlcNAc}_4\text{Man}_3\text{Fuc}_1$), and a $\text{Man}_5\text{GlcNAc}_2$ (m/z 1579) high mannose
400 structure is also observed (Fig. 9B). The Asn-563 N-glycans are much more
401 complex and heterogeneous. Abundant truncated structures at m/z 2081 and
402 2285 have potentially terminal GlcNAc or GalNAc (Fig. 9A). Antennal
403 fucosylation and sialylation is also observed on structures which can
404 assemble sialyl lacNAc, sialyl-Lewis x/a, fucosylated LacdiNAc or sialylated
405 LacdiNAc (GalNAc-GlcNAc), for example peak m/z 4039
406 ($\text{NeuAc}_2\text{Gal}_4\text{GlcNAc}_6\text{Man}_3\text{Fuc}_2$). The presence of m/z 2674
407 ($\text{GalNAc}_2\text{GlcNAc}_4\text{Man}_3\text{Fuc}_3$), in the N297A/C575A mutant confirms the
408 presence of fucosylated LacdiNAc epitopes on the Asn-563 site. Thus,
409 glycosylation at Asn-563 is different to that seen from CHO-K1 cells that
410 assemble less diverse structures without antennal fucosylation and therefore
411 more terminal sialyl-LacNAc (23, 24).

412 The Asn-221 site is mainly composed of bi-antennary complex
413 structures (Fig. 9C). Excluding the base peak, four structures in the C575A
414 background (m/z 2081, 2285, 2459 and 2646) or five structures in the
415 C309L/C575A background (2081, 2285, 2459, 2489 and 2734) could form
416 LacdiNAc antenna (GalNAc-GlcNAc). Antennal fucosylation and sialylation is
417 also observed (Fig. 9C and supplementary Figures).

418 In summary these data show that the types of glycans attached to
419 either Asn-221, Asn-297 or Asn-563 are different between cell lines but are
420 not grossly affected by disulfide bonding.

421
422
423
424

425 ***Fc glycan mutants expressed in HEK 293-F cells are less sialylated than***
426 ***the equivalent mutants expressed in CHO-K1 cells***

427

428 Site-specific levels of sialylation were semi-quantitatively assessed for both
429 panels of mutants and compared to levels seen in the equivalent mutants
430 expressed in CHO-K1 cells (Fig. 10). Although levels of sialylated glycans
431 attached at positions Asn-297 (the N563A/C575A mutant) and Asn-563 (the
432 N297A/C575A mutant) are similar for both cell lines (Fig. 10), a marked
433 reduction in levels of sialylated glycans at Asn-221 (the
434 D221N/N297A/N563A/C575A mutant) is observed when this mutant is
435 expressed in HEK cells (2.8% against 81.8% in CHO, Fig. 10). Removal of
436 Asn-297 generally enhanced levels of sialylation at both Asn-221 and Asn-
437 563, irrespective of the cell line or the multimerization state of the proteins,
438 e.g. compare N297A/C575A vs. C575A and C309L/N297A/C575A vs.
439 C309L/C575A (Fig. 10). The choice of cell line therefore dramatically affects
440 the overall levels of sialylation at individual N-linked attachment sites within
441 the glycan-modified Fc variants.

442

443 ***Asn-221-containing mutants are poor inhibitors of hemagglutination by***
444 ***influenza virus when expressed in HEK 293-F cells***

445

446 To test if the choice of cell line affected the functionality of the two panels of
447 mutant Fcs, we used the World Health Organization (WHO) hemagglutination
448 inhibition assay (HIA) to quantify the inhibitory titers for each mutant against
449 an influenza B virus (Fig. 11). As shown previously with an avian influenza A
450 (H1N1) (24), mutants containing Asn-221 hinge-attached glycans, and in
451 particular the D221N/C309L/N297A/C575A mutant, prevented
452 hemagglutination by an influenza B virus at concentrations as low as 30nM,
453 an eight-fold improvement over equimolar IVIG or polyclonal anti-influenza B
454 antisera (Fig. 11). In stark contrast, the same mutants expressed by HEK 293-
455 F cells were unable to inhibit hemagglutination by either influenza A (not
456 shown) or influenza B virus (Fig. 11). This shows that the functional potential
457 of individual glycan-modified Fc mutants is dependent on the choice of cell
458 line used for their manufacture.

459 **Discussion**

460 We have shown using CHO-K1 cells that the structure and effector function of
461 human IgG1-Fc can be profoundly altered by the addition or removal of N-
462 linked glycosylation (23, 24). For example, we could show that Fc fragments
463 containing complex biantennary glycans attached to both the N- and C-
464 terminal ends of the Fc could inhibit influenza A-mediated agglutination of
465 human erythrocytes (24). The aim of the current study was to reveal possible
466 variation in functional glycosylation related to differences in two host cell lines,
467 CHO-K1 and HEK 293-F, particularly as antibodies and Fc fusions are the
468 fastest growing therapeutic class in the pharmaceutical industry (26, 37, 38).

469 Two intriguing aspects of N-linked glycosylation are relevant to this
470 study. First, the differential binding seen to human glycan (Fig. 5) and Fc γ
471 (Fig. 6) receptors between the same mutants expressed by two different cell
472 lines. These differentially manufactured mutants now need to be compared in
473 relevant *in vivo* disease models where the Fc is therapeutically useful, given
474 that differential sialic acid linkages, α 2,6 and α 2,3, are known to impact on the
475 anti-inflammatory properties of the Fc (39, 40). Such nuanced glycosylation
476 may also explain why the therapeutic efficacy of molecules generated by
477 different expression systems, and subsequently tested in different animal
478 models, do not always translate to efficacy in human studies (41).

479 Second, we have studied the exquisite impact of the host cell line on
480 the efficacy of sialylated Fcs to inhibit influenza viruses (Fig. 11). One
481 possible explanation is that overall sialylation levels for all the influenza
482 blocking mutants, in particular the D221N/C309L/N297A/C575A mutant, are
483 approximately five-fold lower when expressed by HEK 293-F cells (Fig. 10).
484 However, overall level of sialylation is not the only possible explanation for the
485 relative efficacy of the CHO-K1 mutants in inhibiting influenza virus
486 hemagglutination, as the CHO-K1-expressed D221N/C575A mutant also
487 contained approximately five-fold less sialylation than the
488 D221N/C309L/N297A/C575A mutant made in the same cell line (Fig. 10).
489 This indicates that the fine specificity (e.g. α 2,3 vs. α 2,6 linkages) of these
490 sialylated glycans may also be a contributing factor to their efficacy.

491 As demonstrated previously for influenza A (24), binding and inhibition
492 of influenza B viruses is stronger with mutants containing Asn-221, and in
493 particular by the monomeric mutant D221N/C309L/N297A/C575A in which the
494 N- and C-terminal sialylated sugars are spaced $\sim 60\text{\AA}$ apart (Figs. 11 and
495 (24)). Recent biophysical studies with alternative glycan-decorated scaffolds
496 have shown that $\sim 1,000$ fold enhancements over monovalent binding to HA
497 can be achieved with only two sialylated ligands, provided the sugars are
498 arranged 50-100 \AA apart (42, 43). As we also observed with Fc multimerizing
499 mutants from panel 1, no additional benefit with respect to virus neutralization
500 was gained with larger, more complex sialylated structures (Fig. 11, and as
501 seen with the D221N/N297A/N563A/C575A mutant).

502 We do not yet know if sialylated Fcs are susceptible to cleavage by the
503 viral neuraminidase. Although a decoy for NA may be a therapeutically
504 attractive strategy (44), we have not observed a direct decay in the HIA after
505 prolonged incubation. This suggests that the high specific avidity of these
506 molecules for HA may reduce their susceptibility to NA, a hypothesis that fits
507 with the relatively low efficiency of neuraminidase ($k_{\text{cat}} = 30\text{-}155\text{s}^{-1}$), together
508 with the asymmetric distribution of NA in relation to HA on the surface of
509 filamentous influenza viruses (45–47).

510 In order to be useful compounds when administered intranasally, or as
511 an aerosol, the sialylated Fc needs to out-compete sialylated mucins that
512 viruses use through ratchet-like interactions with HA and NA to migrate to the
513 underlying respiratory epithelium (45). Of the 15 known human mucins in the
514 human lung, only MUC5 has been shown to protect from influenza (48, 49).
515 Most sialic acid found on human mucins are O-glycosylated, and where N-
516 linked attachments do occur, these are mostly sialylated via $\alpha 2,6$ -linkages
517 (49). Thus, we were surprised that none of the Fc leads inhibited influenza A
518 (H1N1 propagated in hen eggs) or influenza B (Hong Kong 5/72 propagated
519 in MDCK cells) agglutination of human O⁺ erythrocytes when manufactured by
520 HEK 293-F cells that attach more human type $\alpha 2,6$ -linked sialic acid (Fig. 10).

521 The apparent importance of $\alpha 2,3$ -linked N-glycans to inhibition of both
522 influenza A and B by the CHO-K1 Fc mutants indicates that viruses can
523 evolve away from inhibition by mucus whose predominant O-linked glycans

524 are mostly α 2,6-linked. Our working hypothesis is that HEK-expressed
525 compounds may therefore inhibit influenza viruses that circulate in human
526 populations or that are propagated in cell lines that attach more human-like
527 α 2,6-linked sialic acid.

528 Consequently, by careful consideration of the cell line used in their
529 manufacture, new glycan repertoires with desirable binding attributes and
530 functionality can be imparted to the therapeutically attractive Fc molecule.

531

532

533

534

535

536

537

538

539

540

541

542

543

544

545

546

547

548

549

550

551

552

553

554

555

556

557 **References**

558

- 559 1. Lund, J., N. Takahashi, J. D. Pound, M. Goodall, and R. Jefferis. 1996.
560 Multiple Interactions of IgG with Its Core Oligosaccharide Can Modulate
561 Recognition by Complement and Human Fcγ Receptor I and Influence the
562 Synthesis of Its Oligosaccharide Chains. *J. Immunol.* 157: 4963–4969.
- 563 2. Wright, A., and S. L. Morrison. 1994. Effect of altered CH2-associated
564 carbohydrate structure on the functional properties and in vivo fate of chimeric
565 mouse-human immunoglobulin G1. *J. Exp. Med.* 180: 1087–1096.
- 566 3. Pincetic, A., S. Bournazos, D. J. DiLillo, J. Maamary, T. T. Wang, R.
567 Dahan, B.-M. Fiebiger, and J. V Ravetch. 2014. Type I and type II Fc
568 receptors regulate innate and adaptive immunity. *Nat. Immunol.* 15: 707–716.
- 569 4. Shields, R. L., J. Lai, R. Keck, L. Y. O'Connell, K. Hong, Y. G. Meng, S. H.
570 A. Weikert, and L. G. Presta. 2002. Lack of Fucose on Human IgG1 N-Linked
571 Oligosaccharide Improves Binding to Human FcγRIII and Antibody-
572 dependent Cellular Toxicity . *J. Biol. Chem.* 277: 26733–26740.
- 573 5. Shinkawa, T., K. Nakamura, N. Yamane, E. Shoji-Hosaka, Y. Kanda, M.
574 Sakurada, K. Uchida, H. Anazawa, M. Satoh, M. Yamasaki, N. Hanai, and K.
575 Shitara. 2003. The absence of fucose but not the presence of galactose or
576 bisecting N-acetylglucosamine of human IgG1 complex-type oligosaccharides
577 shows the critical role of enhancing antibody-dependent cellular cytotoxicity.
578 *J. Biol. Chem.* 278: 3466–3473.
- 579 6. Kanda, Y., T. Yamada, K. Mori, A. Okazaki, M. Inoue, K. Kitajima-Miyama,
580 R. Kuni-Kamochi, R. Nakano, K. Yano, S. Kakita, K. Shitara, and M. Satoh.
581 2007. Comparison of biological activity among nonfucosylated therapeutic
582 IgG1 antibodies with three different N-linked Fc oligosaccharides: The high-
583 mannose, hybrid, and complex types. *Glycobiology* 17: 104–118.
- 584 7. Yu, M., D. Brown, C. Reed, S. Chung, J. Lutman, E. Stefanich, A. Wong, J.
585 P. Stephan, and R. Bayer. 2012. Production, characterization and
586 pharmacokinetic properties of antibodies with N-linked Mannose-5 glycans.
587 *MAbs* 4: 475–487.
- 588 8. Goetze, A. M., Y. D. Liu, Z. Zhang, B. Shah, E. Lee, P. V. Bondarenko, and
589 G. C. Flynn. 2011. High-mannose glycans on the Fc region of therapeutic IgG
590 antibodies increase serum clearance in humans. *Glycobiology* 21: 949–959.

- 591 9. Debre, M., M. C. Bonnet, W. H. Fridman, E. Carosella, N. Philippe, P.
592 Reinert, E. Vilmer, C. Kaplan, J. L. Teillaud, and C. Griscelli. 1993. Infusion of
593 Fc gamma fragments for treatment of children with acute immune
594 thrombocytopenic purpura. *Lancet* 342: 945–949.
- 595 10. Liu, L. 2015. Antibody glycosylation and its impact on the
596 pharmacokinetics and pharmacodynamics of monoclonal antibodies and Fc-
597 fusion proteins. *J. Pharm. Sci.* 104: 1866–1884.
- 598 11. Zhang, G., C. A. Massaad, T. Gao, L. Pillai, N. Bogdanova, S. Ghauri, and
599 K. A. Sheikh. 2016. Sialylated intravenous immunoglobulin suppress anti-
600 ganglioside antibody mediated nerve injury. *Exp. Neurol.* 282: 49–55.
- 601 12. Washburn, N., I. Schwab, D. Ortiz, N. Bhatnagar, J. C. Lansing, A.
602 Medeiros, S. Tyler, D. Mekala, E. Cochran, H. Sarvaiya, K. Garofalo, R.
603 Meccariello, J. W. Meador, L. Rutitzky, B. C. Schultes, L. Ling, W. Avery, F.
604 Nimmerjahn, A. M. Manning, G. V. Kaundinya, and C. J. Bosques. 2015.
605 Controlled tetra-Fc sialylation of IVIg results in a drug candidate with
606 consistent enhanced anti-inflammatory activity. *Proc. Natl. Acad. Sci. U. S. A.*
607 112: 201422481.
- 608 13. Anthony, R. M., F. Nimmerjahn, D. J. Ashline, V. N. Reinhold, J. C.
609 Paulson, and J. V. Ravetch. 2008. Recapitulation of IVIG anti-inflammatory
610 activity with a recombinant IgG Fc. *Science (80-)*. 320: 373–376.
- 611 14. Dekkers, G., R. Plomp, C. A. M. Koeleman, R. Visser, H. H. von Horsten,
612 V. Sandig, T. Rispens, M. Wuhrer, and G. Vidarsson. 2016. Multi-level glyco-
613 engineering techniques to generate IgG with defined Fc-glycans. *Sci. Rep.* 6:
614 36964.
- 615 15. Yu, X., K. Baruah, D. J. Harvey, S. Vasiljevic, D. S. Alonzi, B. D. Song, M.
616 K. Higgins, T. A. Bowden, C. N. Scanlan, and M. Crispin. 2013. Engineering
617 hydrophobic protein-carbohydrate interactions to fine-tune monoclonal
618 antibodies. *J. Am. Chem. Soc.* 135: 9723–9732.
- 619 16. Cymer, F., H. Beck, A. Rohde, and D. Reusch. 2018. Therapeutic
620 monoclonal antibody N-glycosylation – Structure, function and therapeutic
621 potential. *Biologicals* 52: 1–11.
- 622 17. Makita, S., and K. Tobinai. 2017. Mogamulizumab for the treatment of T-
623 cell lymphoma. *Expert Opin. Biol. Ther.* 17: 1145–1153.
- 624 18. Huang, W., J. Giddens, S. Q. Fan, C. Toonstra, and L. X. Wang. 2012.

- 625 Chemoenzymatic glycoengineering of intact IgG antibodies for gain of
626 functions. *J. Am. Chem. Soc.* 134: 12308–18.
- 627 19. Yu, X., S. Vasiljevic, D. a. Mitchell, M. Crispin, and C. N. Scanlan. 2013.
628 Dissecting the molecular mechanism of IVIg therapy: The interaction between
629 serum IgG and DC-SIGN is independent of antibody glycoform or Fc domain.
630 *J. Mol. Biol.* 425: 1253–1258.
- 631 20. Mahajan, V. S., and S. Pillai. 2016. Sialic acids and autoimmune disease.
632 *Immunol. Rev.* 269: 145–161.
- 633 21. Subedi, G. P., Q. M. Hanson, and A. W. Barb. 2014. Article Restricted
634 Motion of the Conserved Immunoglobulin G1 N-Glycan Is Essential for
635 Efficient Fc g RIIla Binding. *Struct. Des.* 22: 1478–1488.
- 636 22. Czajkowsky, D. M., J. T. Andersen, A. Fuchs, T. J. Wilson, D. Mekhaie, l,
637 M. Colonna, J. He, Z. Shao, D. A. Mitchell, G. Wu, A. Dell, S. Haslam, K. A.
638 Lloyd, S. C. Moore, I. Sandlie, P. A. Blundell, and R. J. Pleass. 2015.
639 Developing the IVIG biomimetic, Hexa-Fc, for drug and vaccine applications.
640 *Sci. Rep.* 5: 9526.
- 641 23. Blundell, P. A., N. P. L. Le, J. Allen, Y. Watanabe, and R. J. Pleass. 2017.
642 Engineering the fragment crystallizable (Fc) region of human IgG1 multimers
643 and monomers to fine-tune interactions with sialic acid-dependent receptors.
644 *J. Biol. Chem.* 292: 12994–13007.
- 645 24. Blundell, P. A., D. Lu, M. Wilkinson, A. Dell, S. Haslam, and R. J. Pleass.
646 2019. Insertion of N-Terminal Hinge Glycosylation Enhances Interactions of
647 the Fc Region of Human IgG1 Monomers with Glycan-Dependent Receptors
648 and Blocks Hemagglutination by the Influenza Virus. *J. Immunol.* 202: 1595–
649 1611.
- 650 25. Spence, S., M. K. Greene, F. Fay, E. Hams, S. P. Saunders, U. Hamid, M.
651 Fitzgerald, J. Beck, B. K. Bains, P. Smyth, E. Themistou, D. M. Small, D.
652 Schmid, C. M. O’Kane, D. C. Fitzgerald, S. M. Abdelghany, J. A. Johnston, P.
653 G. Fallon, J. F. Burrows, D. F. McAuley, A. Kissenpfennig, and C. J. Scott.
654 2015. Targeting Siglecs with a sialic acid-decorated nanoparticle abrogates
655 inflammation. *Sci. Transl. Med.* 7: 1–13.
- 656 26. Walsh, G. 2018. Biopharmaceutical benchmarks 2018. *Nat. Biotechnol.*
657 36: 1136–1145.
- 658 27. Goh, J. B., and S. K. Ng. 2018. Impact of host cell line choice on glycan

- 659 profile. *Crit. Rev. Biotechnol.* 38: 851–867.
- 660 28. Ghaderi, D., R. E. Taylor, V. Padler-Karavani, S. Diaz, and A. Varki. 2010.
- 661 Implications of the presence of N-glycolylneuraminic acid in recombinant
- 662 therapeutic glycoproteins. *Nat. Biotechnol.* 28: 863–867.
- 663 29. Mulligan, M. S., R. L. Warner, C. W. Rittershaus, L. J. Thomas, U. S.
- 664 Ryan, K. E. Foreman, L. D. Crouch, G. O. Till, and P. A. Ward. 1999.
- 665 Endothelial targeting and enhanced antiinflammatory effects of complement
- 666 inhibitors possessing sialyl Lewis(x) moieties. *J. Immunol.* 162: 4952–4959.
- 667 30. Czajkowsky, D. M., J. T. Andersen, A. Fuchs, T. J. Wilson, D. Mekhaieel,
- 668 M. Colonna, J. He, Z. Shao, D. a. Mitchell, G. Wu, A. Dell, S. Haslam, K. a.
- 669 Lloyd, S. C. Moore, I. Sandlie, P. a. Blundell, and R. J. Pleass. 2015.
- 670 Developing the IVIG biomimetic, Hexa-Fc, for drug and vaccine applications.
- 671 *Sci. Rep.* 5: 9526.
- 672 31. Mekhaieel, D. N. A., D. M. Czajkowsky, J. T. Andersen, J. Shi, M. El-
- 673 Faham, M. Doenhoff, R. S. McIntosh, I. Sandlie, J. He, J. Hu, Z. Shao, and R.
- 674 J. Pleass. 2011. Polymeric human Fc-fusion proteins with modified effector
- 675 functions. *Sci. Rep.* 1: 1–11.
- 676 32. North, S. J., J. Jang-Lee, R. Harrison, K. Canis, M. N. Ismail, A. Trollope,
- 677 A. Antonopoulos, P. C. Pang, P. Grassi, S. Al-Chalabi, A. T. Etienne, A. Dell,
- 678 and S. M. Haslam. 2010. Mass spectrometric analysis of mutant mice.
- 679 *Methods Enzymol.* 478: 27–77.
- 680 33. Ceroni, A., K. Maass, H. Geyer, R. Geyer, A. Dell, and S. M. Haslam.
- 681 2008. GlycoWorkbench: A tool for the computer-assisted annotation of mass
- 682 spectra of glycans. *J. Proteome Res.* 7: 1650–1659.
- 683 34. Massoud, A. H., M. Yona, D. Xue, F. Chouiali, H. Alturaihi, A. Ablona, W.
- 684 Mourad, C. A. Piccirillo, and B. D. Mazer. 2014. Dendritic cell
- 685 immunoreceptor: A novel receptor for intravenous immunoglobulin mediates
- 686 induction of regulatory T cells. *J. Allergy Clin. Immunol.* 133: 853–863.
- 687 35. Seite, J. F., D. Cornec, Y. Renaudineau, P. Youinou, R. A. Mageed, and
- 688 S. Hillion. 2010. IVIg modulates BCR-signaling through CD22 and promotes
- 689 apoptosis in mature human B lymphocytes. *Blood* 116: 1686–1704.
- 690 36. Lo, C. Y., A. Antonopoulos, R. Gupta, J. Qu, A. Dell, S. M. Haslam, and S.
- 691 Neelamegham. 2013. Competition between core-2 GlcNAc-transferase and
- 692 ST6GalNAc-transferase regulates the synthesis of the leukocyte selectin

- 693 ligand on human P-selectin glycoprotein ligand-1. *J. Biol. Chem.* 288: 13974–
694 13987.
- 695 37. Mastrangeli, R., W. Palinsky, and H. Bierau. 2018. Glycoengineered
696 antibodies: towards the next-generation of immunotherapeutics. *Glycobiology*
697 29: 199–210.
- 698 38. Czajkowsky, D. M., J. Hu, Z. Shao, and R. J. Pleass. 2012. Fc-fusion
699 proteins: New developments and future perspectives. *EMBO Mol. Med.* 4:
700 1015–1028.
- 701 39. Sondermann, P., A. Pincetic, J. Maamary, K. Lammens, and J. V Ravetch.
702 2013. General mechanism for modulating immunoglobulin effector function.
703 *Proc. Natl. Acad. Sci.* 110: 9868–9872.
- 704 40. Anthony, R. M., F. Wermeling, M. C. I. Karlsson, and J. V Ravetch. 2008.
705 Identification of a receptor required for the anti-inflammatory activity of IVIG.
706 *Proc. Natl. Acad. Sci. U. S. A.* 105: 19571–8.
- 707 41. Antonopoulos, A., S. J. North, S. M. Haslam, and A. Dell. 2012.
708 Glycosylation of mouse and human immune cells: insights emerging from N-
709 glycomics analyses. *Biochem. Soc. Trans.* 39: 1334–1340.
- 710 42. Bandlow, V., D. Lauster, K. Ludwig, M. Hilsch, V. Reiter-Scherer, J. P.
711 Rabe, C. Böttcher, A. Herrmann, and O. Seitz. 2019. Sialyl-LacNAc-PNA·DNA
712 Concatamers by Rolling-Circle Amplification as Multivalent Inhibitors of
713 Influenza A Virus Particles. *ChemBioChem* 20: 1–8.
- 714 43. Bandlow, V., S. Liese, D. Lauster, K. Ludwig, R. R. Netz, A. Herrmann,
715 and O. Seitz. 2017. Spatial Screening of Hemagglutinin on Influenza A Virus
716 Particles: Sialyl-LacNAc Displays on DNA and PEG Scaffolds Reveal the
717 Requirements for Bivalency Enhanced Interactions with Weak Monovalent
718 Binders. *J. Am. Chem. Soc.* 139: 16389–16397.
- 719 44. Ernst, B., and J. L. Magnani. 2009. From carbohydrate leads to
720 glycomimetic drugs. *Nat. Rev. Drug Discov.* 8: 661–677.
- 721 45. Vahey, M. D., and D. A. Fletcher. 2019. Influenza A virus surface proteins
722 are organized to help penetrate host mucus. *Elife* 8: e43764.
- 723 46. Waldmann, M., R. Jirmann, K. Hoelscher, M. Wienke, F. C. Niemeyer, D.
724 Rehders, and B. Meyer. 2014. A nanomolar multivalent ligand as entry
725 inhibitor of the hemagglutinin of avian influenza. *J. Am. Chem. Soc.* 136: 783–
726 788.

- 727 47. Gao, Z., M. Niikura, and S. G. Withers. 2017. Ultrasensitive Fluorogenic
728 Reagents for Neuraminidase Titration. *Angew. Chemie - Int. Ed.* 56: 6112–
729 6116.
- 730 48. Roy, M. G., A. Livraghi-Butrico, A. A. Fletcher, M. M. McElwee, S. E.
731 Evans, R. M. Boerner, S. N. Alexander, L. K. Bellinghausen, A. S. Song, Y. M.
732 Petrova, M. J. Tuvim, R. Adachi, I. Romo, A. S. Bordt, M. G. Bowden, J. H.
733 Sisson, P. G. Woodruff, D. J. Thornton, K. Rousseau, M. M. De La Garza, S.
734 J. Moghaddam, H. Karmouty-Quintana, M. R. Blackburn, S. M. Drouin, C. W.
735 Davis, K. A. Terrell, B. R. Grubb, W. K. O'Neal, S. C. Flores, A. Cota-Gomez,
736 C. A. Lozupone, J. M. Donnelly, A. M. Watson, C. E. Hennessy, R. C. Keith, I.
737 V. Yang, L. Barthel, P. M. Henson, W. J. Janssen, D. A. Schwartz, R. C.
738 Boucher, B. F. Dickey, and C. M. Evans. 2014. Muc5b is required for airway
739 defence. *Nature* 505: 412–416.
- 740 49. Zanin, M., P. Baviskar, R. Webster, and R. Webby. 2016. The Interaction
741 between Respiratory Pathogens and Mucus. *Cell Host Microbe* 19: 159–168.

742

743 **Acknowledgements**

744 We thank Abzena PLC for running the surface plasmon resonance analysis
745 and Dr Mark Wilkinson for running SE-HPLC samples.

746

747 **Author contributions**

748 R.J.P. conceived and designed the overall study. R.J.P, P.A.B., D.L., AD and
749 SMH designed and performed experiments. R.J.P. wrote the manuscript, and
750 all authors commented on drafts and reviewed the final manuscript.

751

752 **Disclosures**

753 R.J.P. and P.A.B. declare that work discussed within is subject to ongoing
754 patent applications.

755

756

757

758

759

760

761 **Legends**

762

763 **FIGURE 1.** Schematic showing the various hexa-Fc glycan mutants in which
764 Cys-575 is mutated to alanine to create the C575A panel of mutants. Stars
765 indicate the hinge Asn-221, the C γ 2 Asn-297, and the tailpiece Asn-563
766 glycan sites respectively.

767

768 **FIGURE 2.** Schematic showing the C575A panel of glycan mutants from Fig.
769 1 in which the which Cys-309 and Leu-310 are changed to leucine and
770 histidine, as found in the native IgG1 Fc sequence to create the C309L/C575A
771 panel of mutants. Stars indicate the hinge Asn-221, the C γ 2 Asn-297, and the
772 tailpiece Asn-563 glycan sites.

773

774 **FIGURE 3.** Characterization of mutant Fc proteins by SDS-PAGE. **(A)** Cys-
775 309 competent mutants in which Cys-575 is mutated to alanine to create the
776 C575A panel of mutants. Mutants with N563A run as ladderred multimers.
777 Insufficient material was obtained with N297A/N563A/C575A for further
778 analysis. The addition of the N-X-(T/S) glycan sequon to generate N-
779 terminally glycosylated hinges (the D221N series of mutants) did not affect
780 multimerization but rather increased the molecular mass of all mutants. The
781 N297A mutants run as monomers, dimers and trimers. **(B)** the same mutants
782 as in (A) but run under reducing conditions. The D221N/C575A mutant has
783 the largest mass because it has three glycans attached. The types of glycans
784 attached at Asn-221, Asn-297, and Asn-563 for all the mutants are shown in
785 Fig. 9 and supplemental figures. The decreasing molecular masses seen in
786 the Fc represent the sequential loss of N-linked glycans. **(C)** The same
787 mutants as in (A) but stained with Coomassie reagent. **(D)** Substitution of
788 Cys-309 with leucine onto the C575A mutants shown in (A) to create the
789 double cysteine knockouts, which all run as monomers. C309L in which Cys-
790 575 is present also multimerizes. **(E)** The same mutants as in (D) but run
791 under reducing conditions. Note that the D221N/C309L/C575A mutant with
792 three glycan sites has the largest mass, as seen with the equivalent mutant
793 D221N/C575A in panel (A). **(F)** Coomassie-stained gel of (D). All proteins

794 were run under either non-reducing (panels A and D) or reducing conditions
795 (panels B and E) at 2 µg protein per lane on 4-8% acrylamide gradient gels,
796 transferred to nitrocellulose, and blotted with anti-human IgG Fc (Sigma-
797 Aldrich).

798

799 **FIGURE 4.** Size-exclusion chromatography analysis of Fc mutants expressed
800 in HEK 293-F cells. (A) The C575A panel of mutants. (B) The C309L/C575A
801 panel of mutants. Boxed chromatograms represent profiles for equivalent
802 mutants expressed in CHO-K1 cells, as published previously (24).

803

804 **FIGURE 5.** Shading matrix showing the differential binding of HEK 293-F or
805 CHO-K1 mutant proteins to recombinant glycan receptors. Results from at
806 least two independent ELISA experiments are expressed as fold change (up
807 or down) with respect to the internal IgG1 Fc control run on each plate.
808 Standalone ELISA data are provided in the supplementary figures. White
809 boxes = not tested.

810

811 **FIGURE 6.** Shading matrix showing the differential binding of HEK 293-F or
812 CHO-K1 mutant proteins to recombinant Fcγ receptors. Results from at least
813 two independent ELISA experiments are expressed as fold change (up or
814 down) with respect to the internal IgG1 Fc control run on each plate.
815 Standalone ELISA data are provided in the supplementary figures.

816

817 **FIGURE 7.** Surface plasmon resonance analysis. Binding of selected mutants
818 to human FcγRIIIB (panels **A-C**) or FcγRIIA-Arg¹⁶⁷ (panels **D-F**) by Biacore.
819 Control IgG1 Fc (panels **A,D**) is compared to C309L/N563A/C575A (panels
820 **B,E**) and D221N/C309L/N563A/C575A (panels **C,F**). Curves show doubling
821 dilutions from the highest indicated concentration of protein. Because of the
822 varying stoichiometry of the molecules shown (as seen in Figs. 3 and 4), an
823 accurate determination of the interaction kinetics is not possible. Binding was
824 to receptors sourced from R&D systems (Bio-Techne).

825

826

827 **FIGURE 8.** Binding of selected C575A and C309L/C575A mutants to
828 complement component C1q. Mutants expressed in HEK 293-F cells bind
829 human C1q better than the equivalent mutants expressed in CHO-K1 cells.
830 Compare for example the D221N/C575 mutant made in CHO-K1 cells (open
831 triangle) against the same mutant made in HEK 293-F cells (open circle) and
832 compared on the same plate. Error bars represent standard deviations around
833 the mean value, n=2 independent ELISA experiments.

834

835 **FIGURE 9.** MALDI-TOF MS profiles of permethylated N-glycans from the
836 N297A/C575A (A), N563A/C575A (B), and D221N/N297A/N563A/C575A (C)
837 Fc glycan mutants. Linkage determined monosaccharides are positioned
838 above the bracket on a structure. Poly-hexose contaminants are highlighted
839 with crosses. The data were acquired in the positive ion mode to observe
840 $[M+Na]^+$ molecular ions. All the structures are based on composition and
841 knowledge of N-glycan biosynthetic pathways. Structures shown outside a
842 bracket have not had their antenna location unequivocally defined.

843

844 **FIGURE 10.** Semi-quantitative determination of sialylated (purple) against
845 neutral (grey) glycans from the C575A and C309L/C575A mutants
846 expressed in CHO-K1 or HEK 293-F cells. Values shown in brackets under
847 the names of each mutant show percentage sialylated structures as
848 determined from summed intensities.

849

850 **FIGURE 11.** Impact of Fc glycosylation on influenza B-mediated
851 hemagglutination. Mutant Fcs manufactured in either HEK 293-F or CHO-K1
852 cells were compared to equimolar concentration of IVIG or polyclonal anti-
853 influenza B antibodies at inhibiting virus-mediated agglutination of human
854 erythrocytes. 1. L309C, 2. C575A, 3. N297A/C575A, 4. N563A/C575A, 5. no
855 protein, 6. D221N/C575A, 7. D221N/N297A/C575A, 8. D221N/N563A/C575A,
856 9. D221N/N297A/N563A/C575A, 10. C309L, 11. C309L/C575A, 12.
857 C309L/N297A/C575A, 13. C309L/N575A/C575A, 14.
858 C309L/N297A/N563A/C575A, 15. D221N/C309L/C575A, 16.
859 D221N/C309L/N297A/C575A, 17. D221N/C309L/N563A/C575A, 18.
860 D221N/C309L/N297A/N563A/C575A. A constant amount of influenza B Hong-

861 Kong 5/72 virus was incubated with titrated amounts of the Fc glycan mutants
862 and added to human O+ erythrocytes that were then allowed to sediment at
863 room temperature for 1h. Non-agglutinated RBCs form a small halo. n=3
864 independent experiments.

Fig. 1


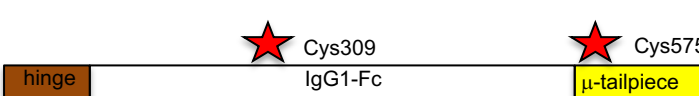
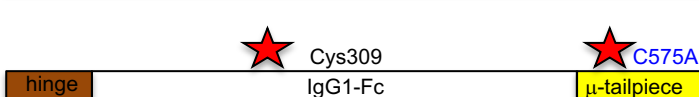
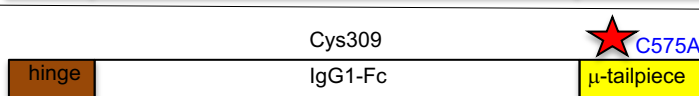
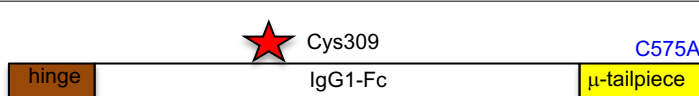
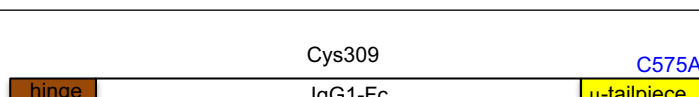
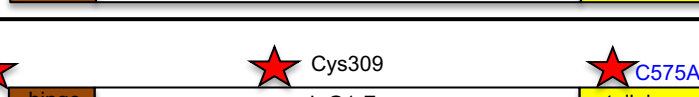
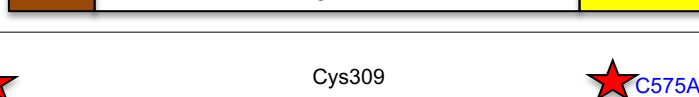
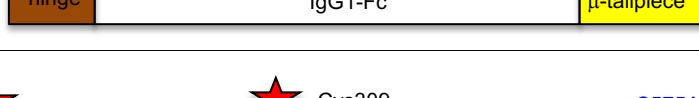
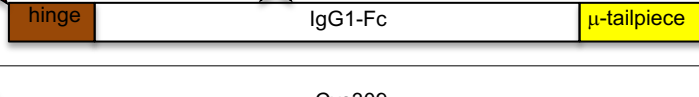
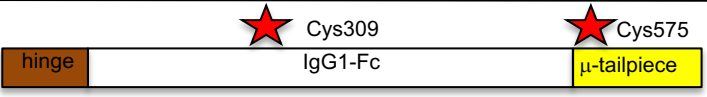
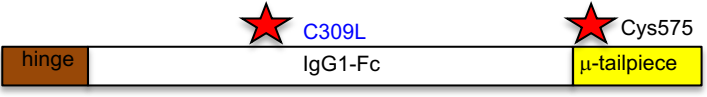

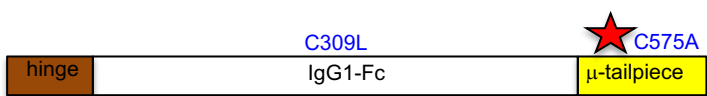
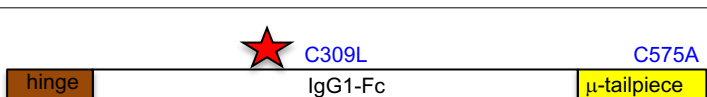
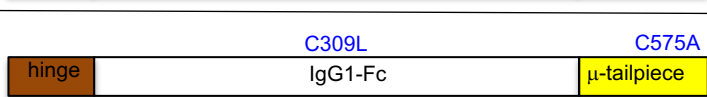
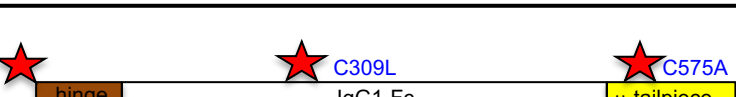

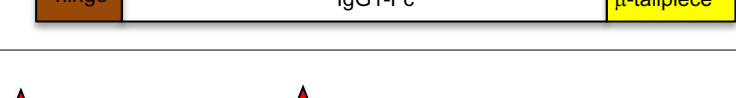
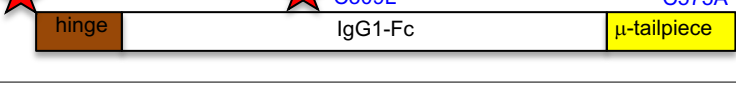
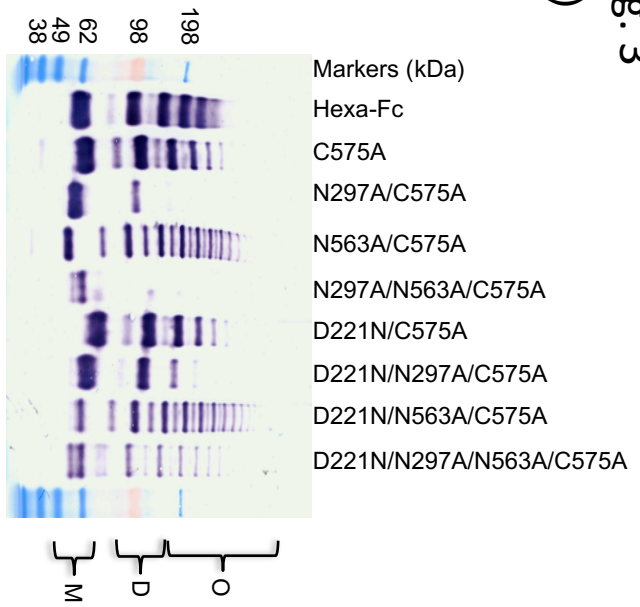
Fc-construct	Heavy chain composition	CHO-K1 PAGE	CHO-K1 HPLC	HEK-293 PAGE	HEK-293 HPLC
IgG1-Fc		monomer	monomer	monomer	monomer
Hexa-Fc		multimer	multimer	multimer	multimer
C575A		monomer >dimer >trimer	monomer >dimer	multimer	multimer
N297A/C575A		monomer >dimer >trimer	monomer >dimer	monomer >dimer	monomer
N563A/C575A		multimer	multimer	multimer	multimer
N297A/N563A/ C575A		multimer	multimer	No protein (monomer by blotting)	No protein
D221N/C575A		monomer >dimer	monomer >dimer	multimer	multimer
D221N/N297A/ C575A		monomer >dimer	monomer	monomer >dimer >trimer	monomer
D221N/N563A/ C575A		multimer	multimer	multimer	monomer & multimer
D221N/N297A/ N563A/C575A		multimer	multimer	multimer	monomer & multimer

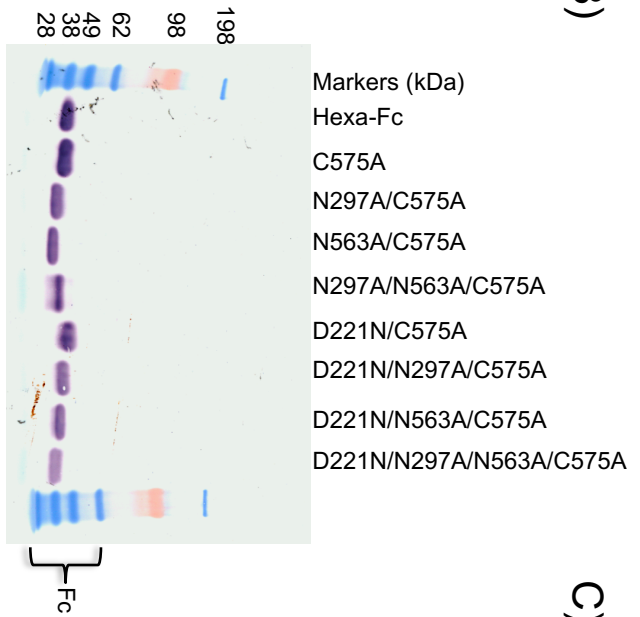
Fig.2

Fc-construct	Heavy chain composition	CHO-K1 PAGE	CHO-K1 HPLC	HEK-293 PAGE	HEK-293 HPLC
Hexa-Fc		multimer	multimer	multimer	multimer
C309L		multimer	multimer	monomer >multimers	monomer
C309L/C575A		monomer	monomer	monomer >>dimer	monomer
C309L/N297A/ C575A		monomer	monomer	monomer	monomer
C309L/N563A/ C575A		monomer	multimer	monomer	monomer >dimer >trimer
C309L/N297A/ N563A/C575A		monomer	multimer	monomer	monomer >dimer >trimer
D221N/C309L/ C575A		monomer	monomer	monomer	monomer
D221N/C309L/ N297A/C575A		monomer	monomer	monomer	monomer
D221N/C309L/ N563A/C575A		monomer >dimer	multimer	monomer	monomer dimer multimer
D221N/C309L/ N297A/N563A/ C575A		monomer	monomer multimer >dimer	monomer	monomer dimer multimer

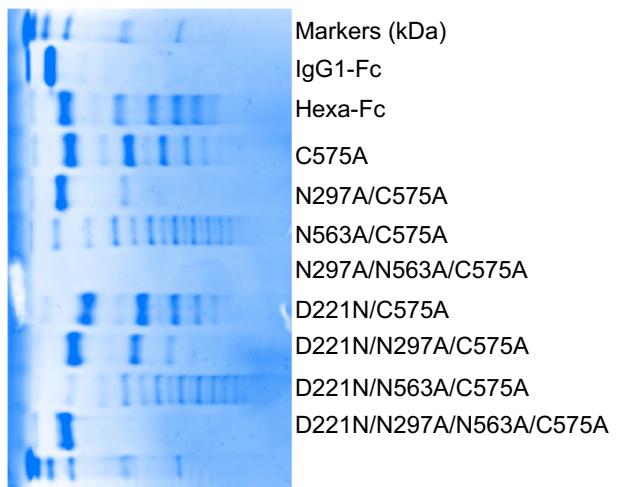
A)



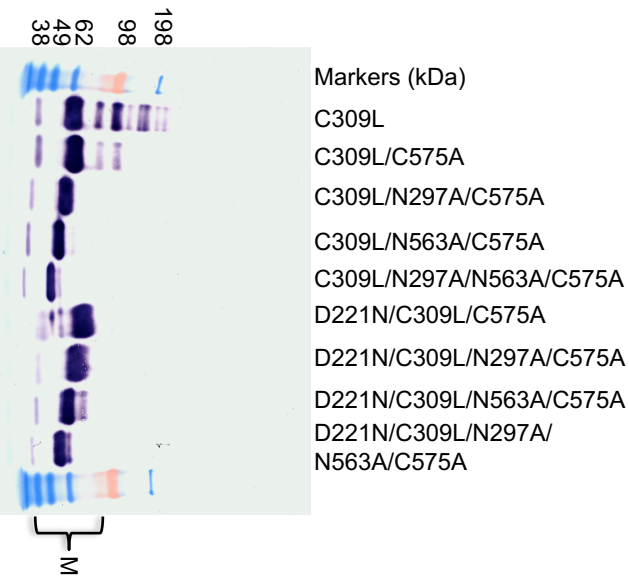
B)



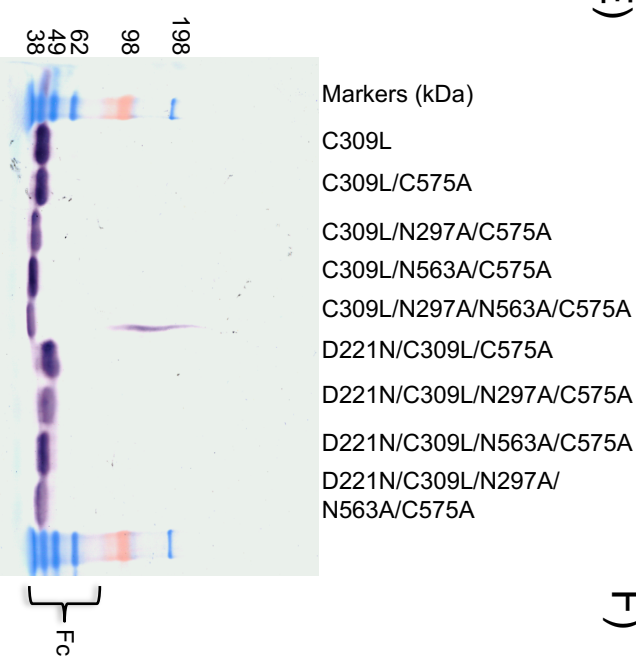
C)



D)



E)



F)

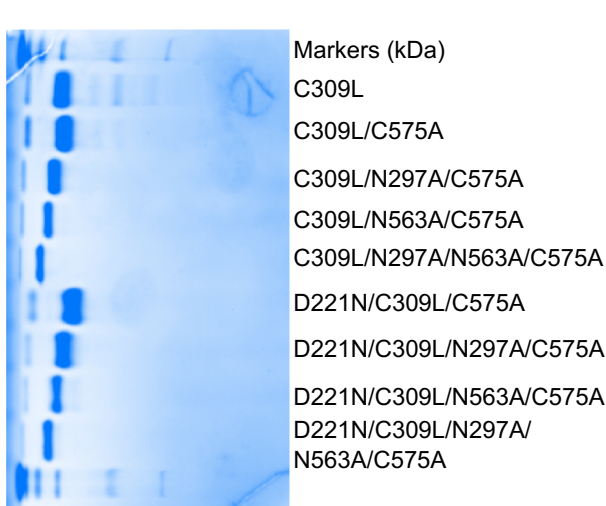
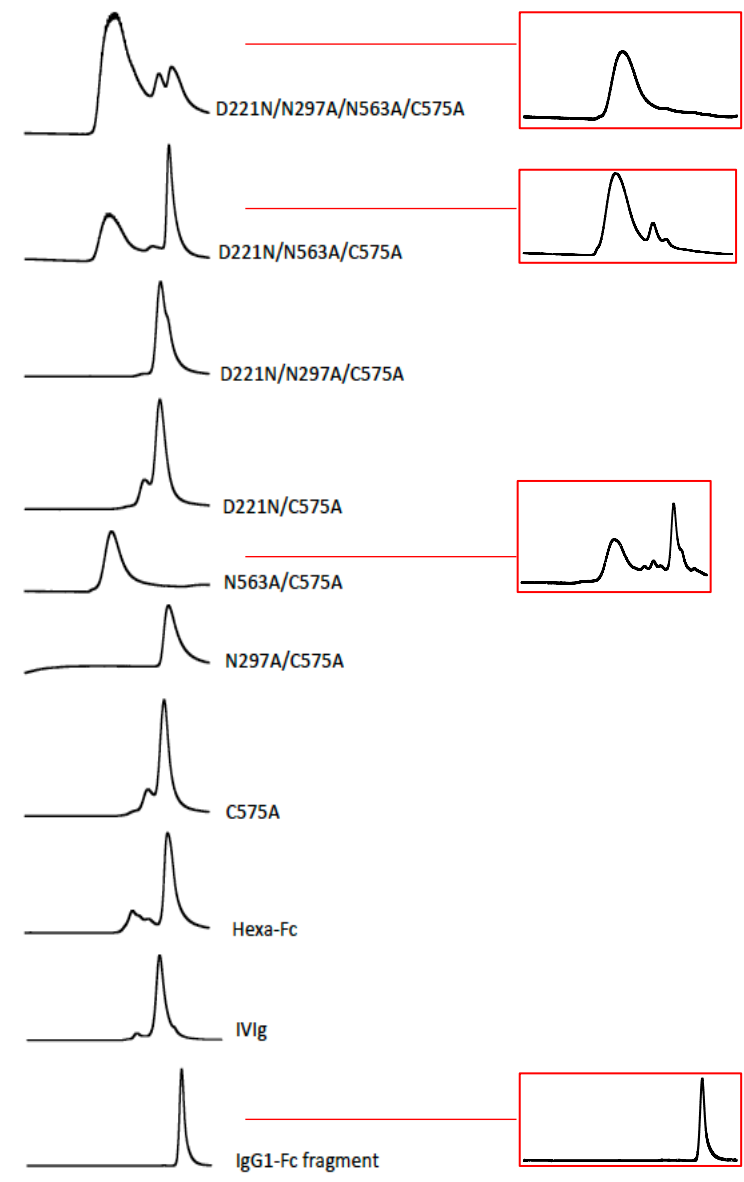
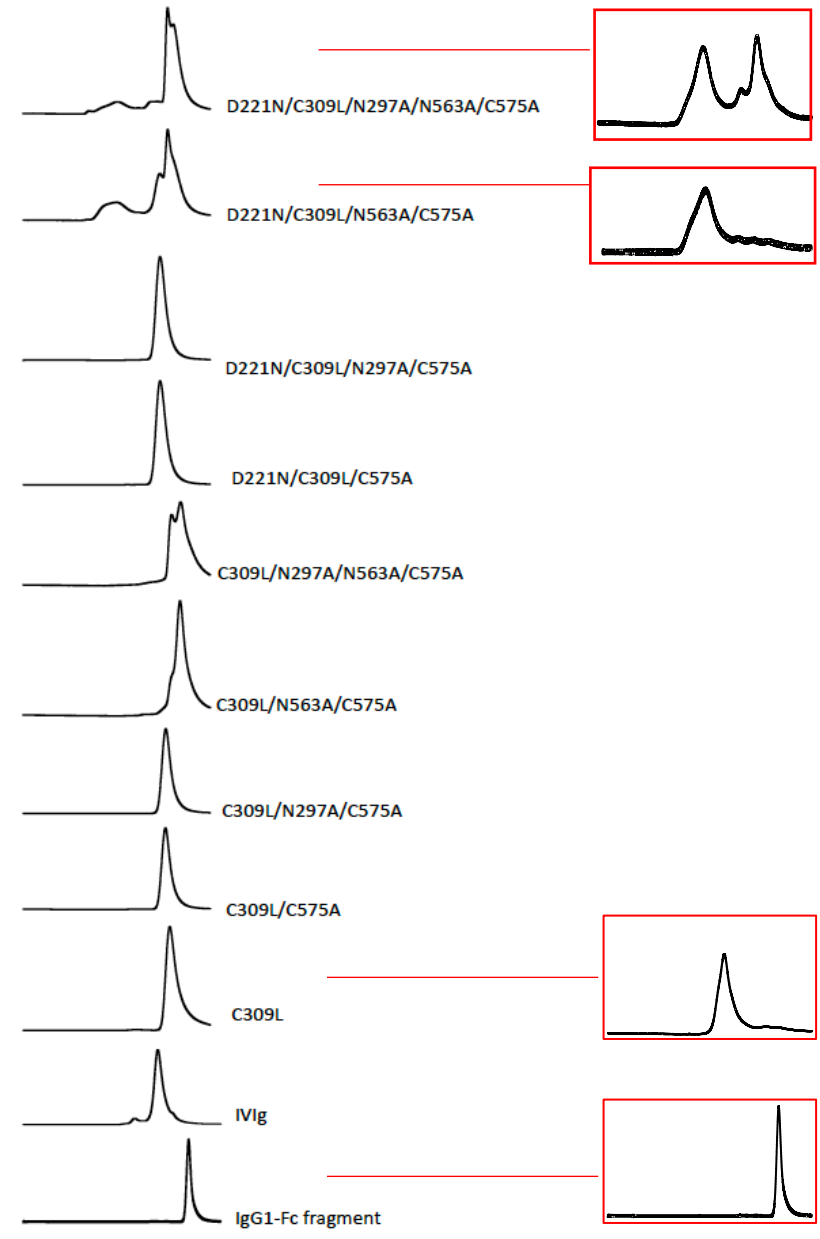


Fig. 4

A)



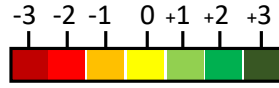
B)



CHO-K1

HEK

Fig. 5



Panel 1 mutants

Hexa-Fc
 C575A
 N297A/C575A
 N563A/C575A
 N297A/N563A/C575A
 D221N/C575A
 D221N/N297A/C575A
 D221N/N563A/C575A
 D221N/N297A/N563A/C575A

Panel 2 mutants

C309L
 C309L/C575A
 C309L/N297A/C575A
 C309L/N563A/C575A
 C309L/N297A/N563A/C575A
 D221N/C309L/C575A
 D221N/C309L/N297A/C575A
 D221N/C309L/N563A/C575A
 D221N/C309L/N297A/N563A/C575A

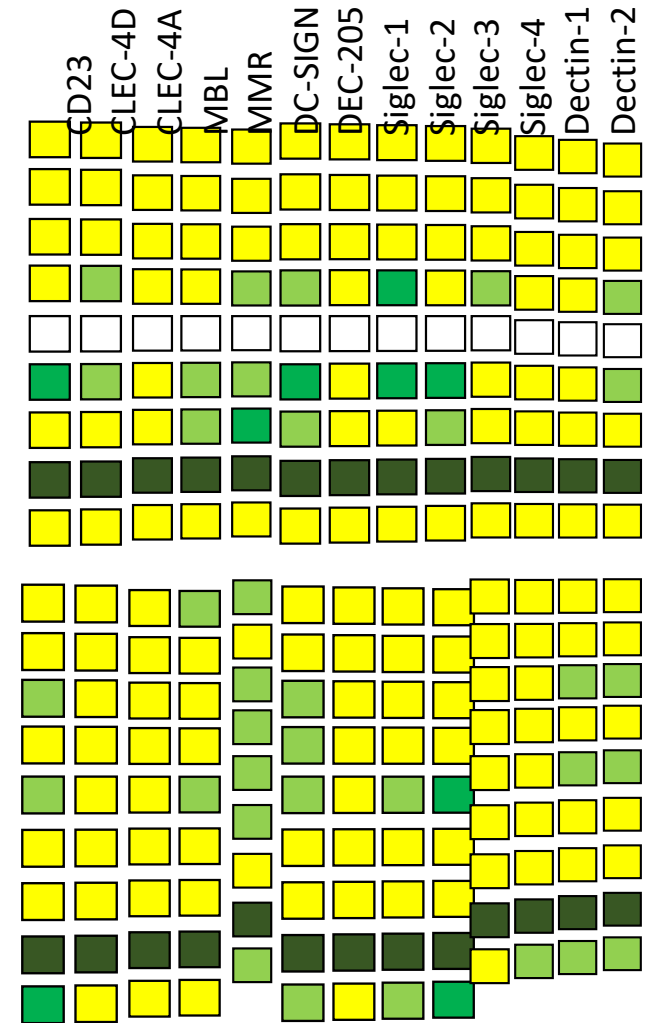
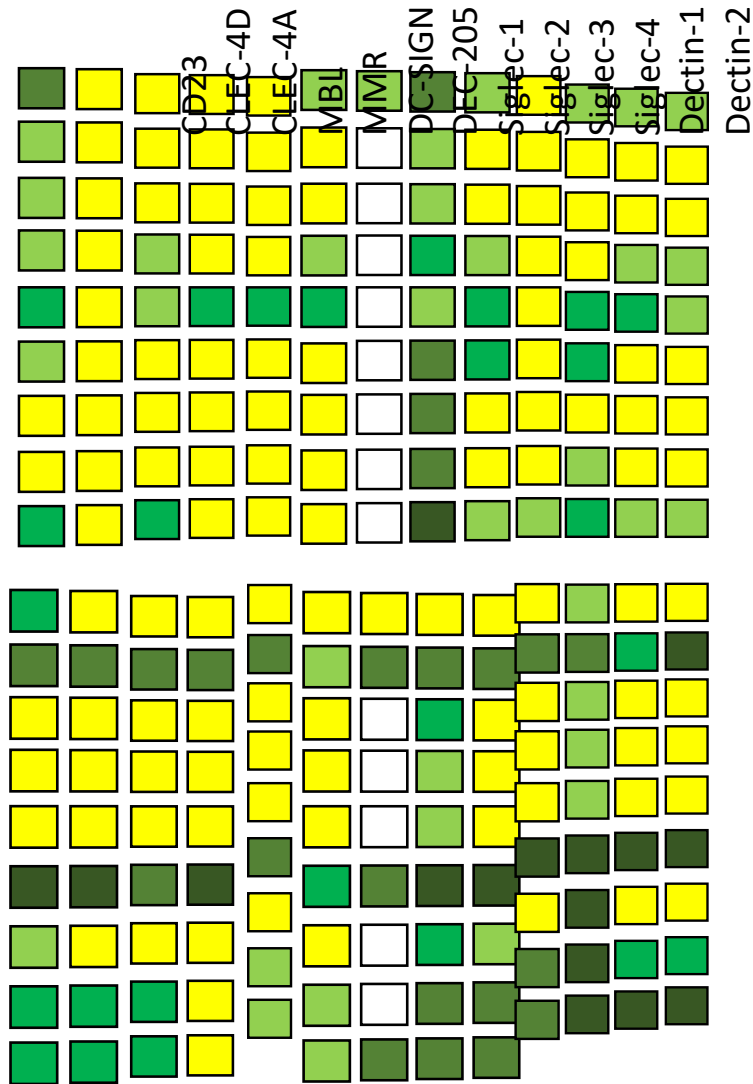
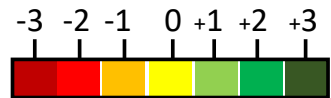


Fig. 6



Panel 1 mutants

Hexa-Fc
 C575A
 N297A/C575A
 N563A/C575A
 N297A/N563A/C575A
 D221N/C575A
 D221N/N297A/C575A
 D221N/N563A/C575A
 D221N/N297A/N563A/C575A

Panel 2 mutants

C309L
 C309L/C575A
 C309L/N297A/C575A
 C309L/N563A/C575A
 C309L/N297A/N563A/C575A
 D221N/C309L/C575A
 D221N/C309L/N297A/C575A
 D221N/C309L/N563A/C575A
 D221N/C309L/N297A/N563A/C575A

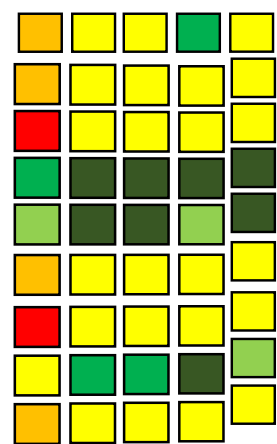
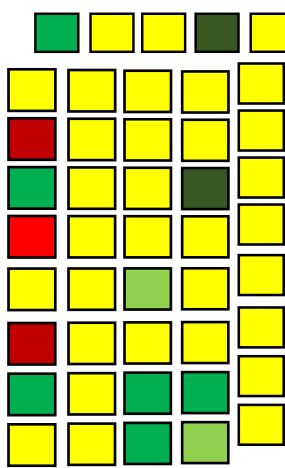
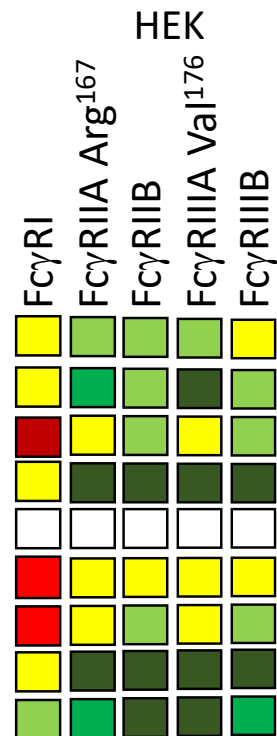
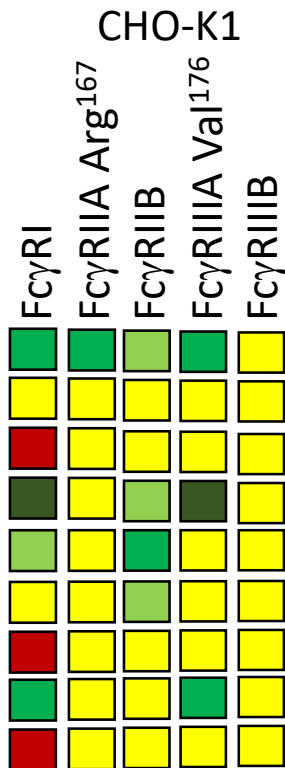


Fig. 7

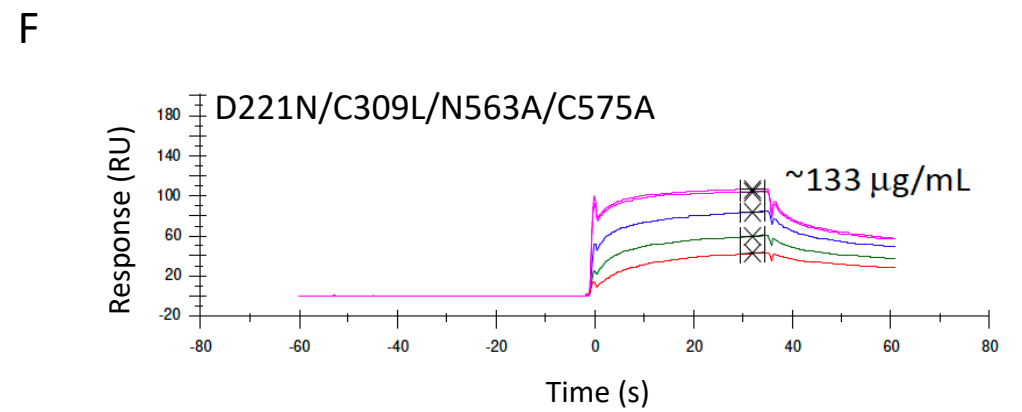
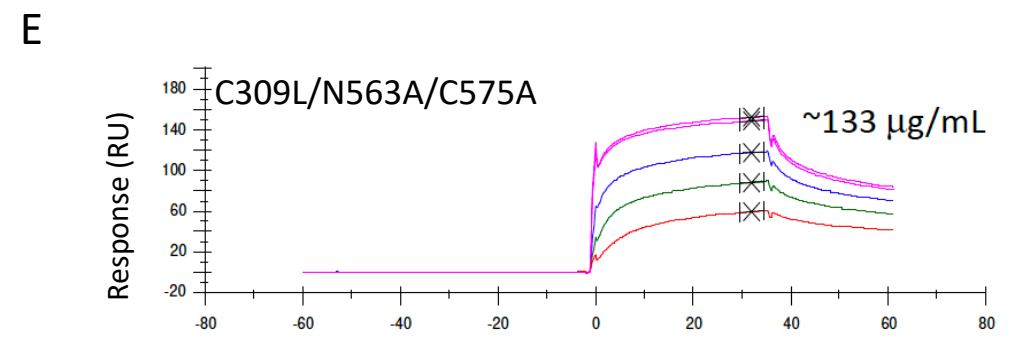
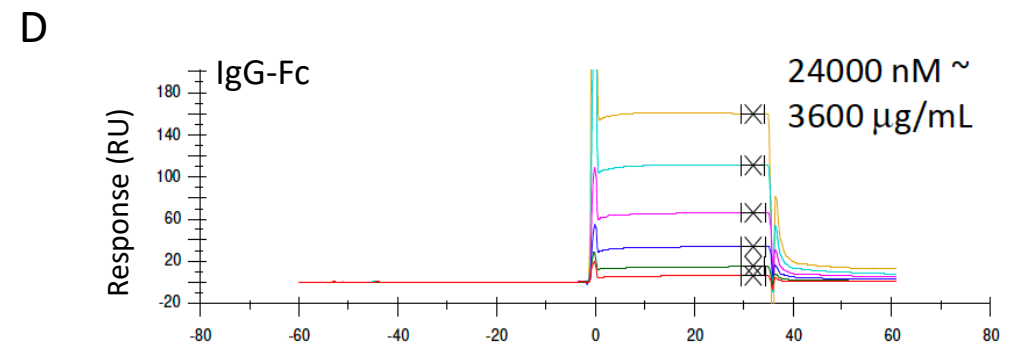
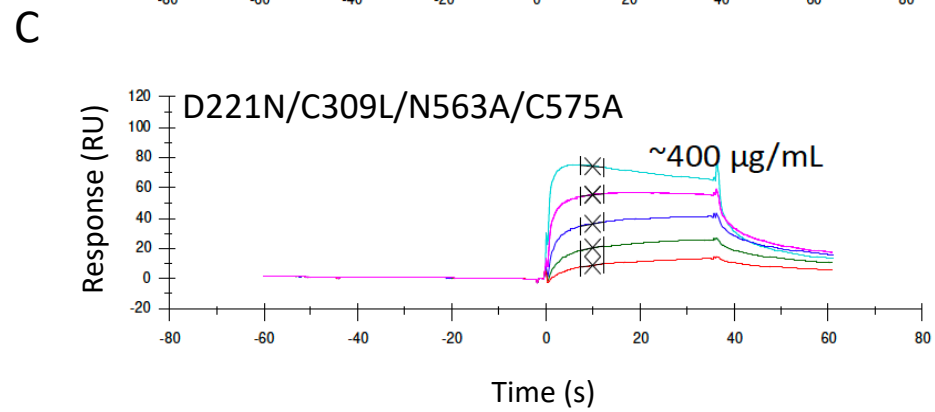
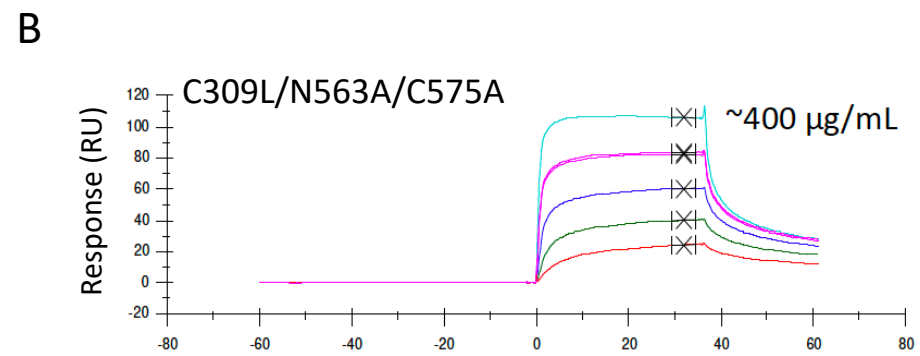
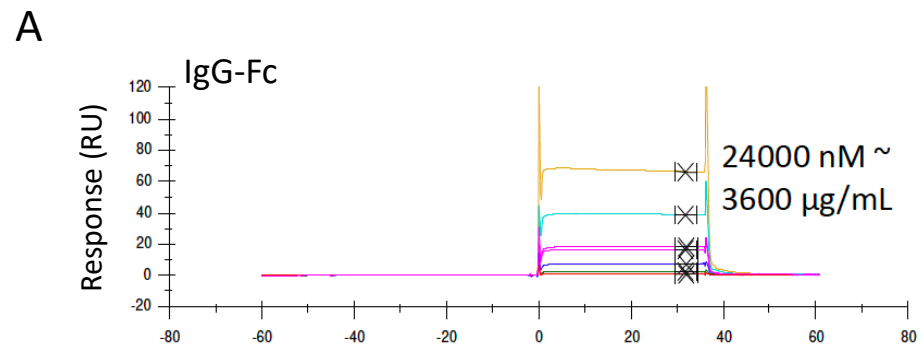


Fig. 8

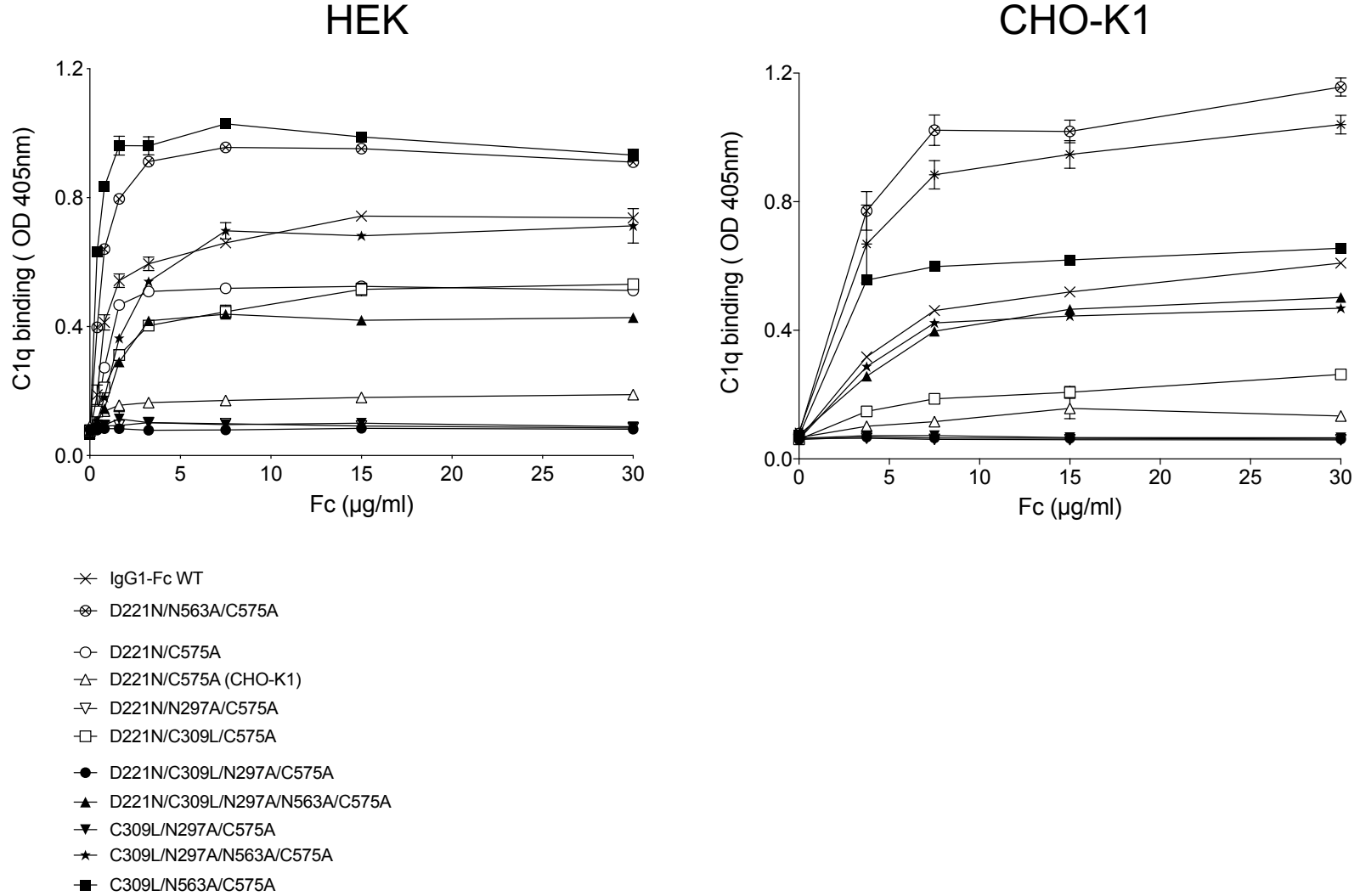


Fig. 9

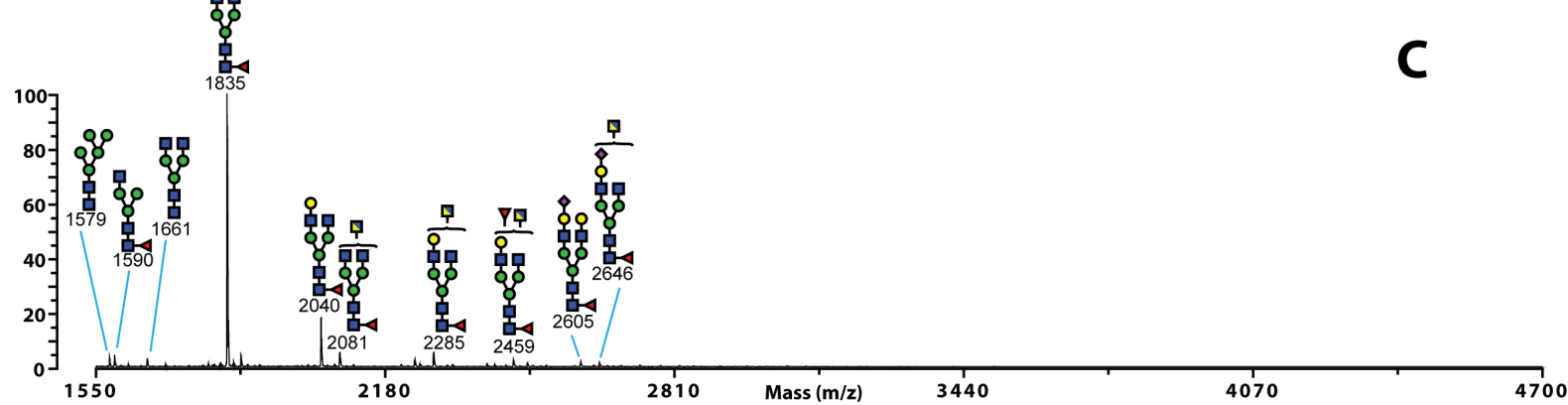
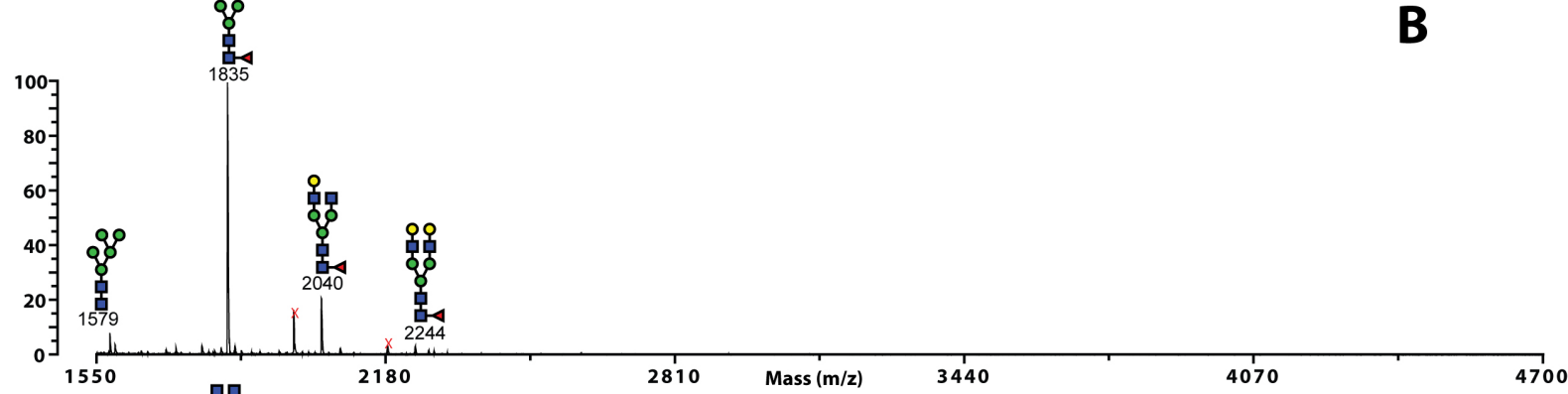
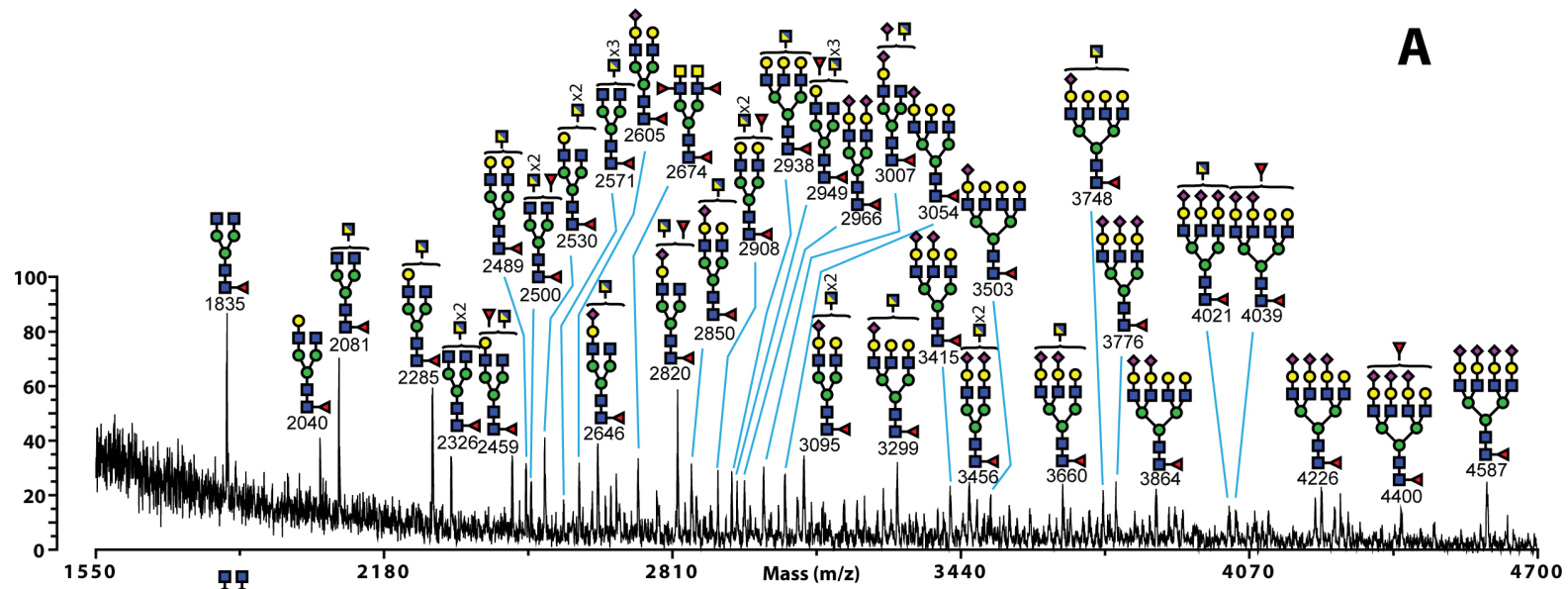


Fig. 10

CHO

HEK

Panel 1

Panel 2

Panel 1

Panel 2

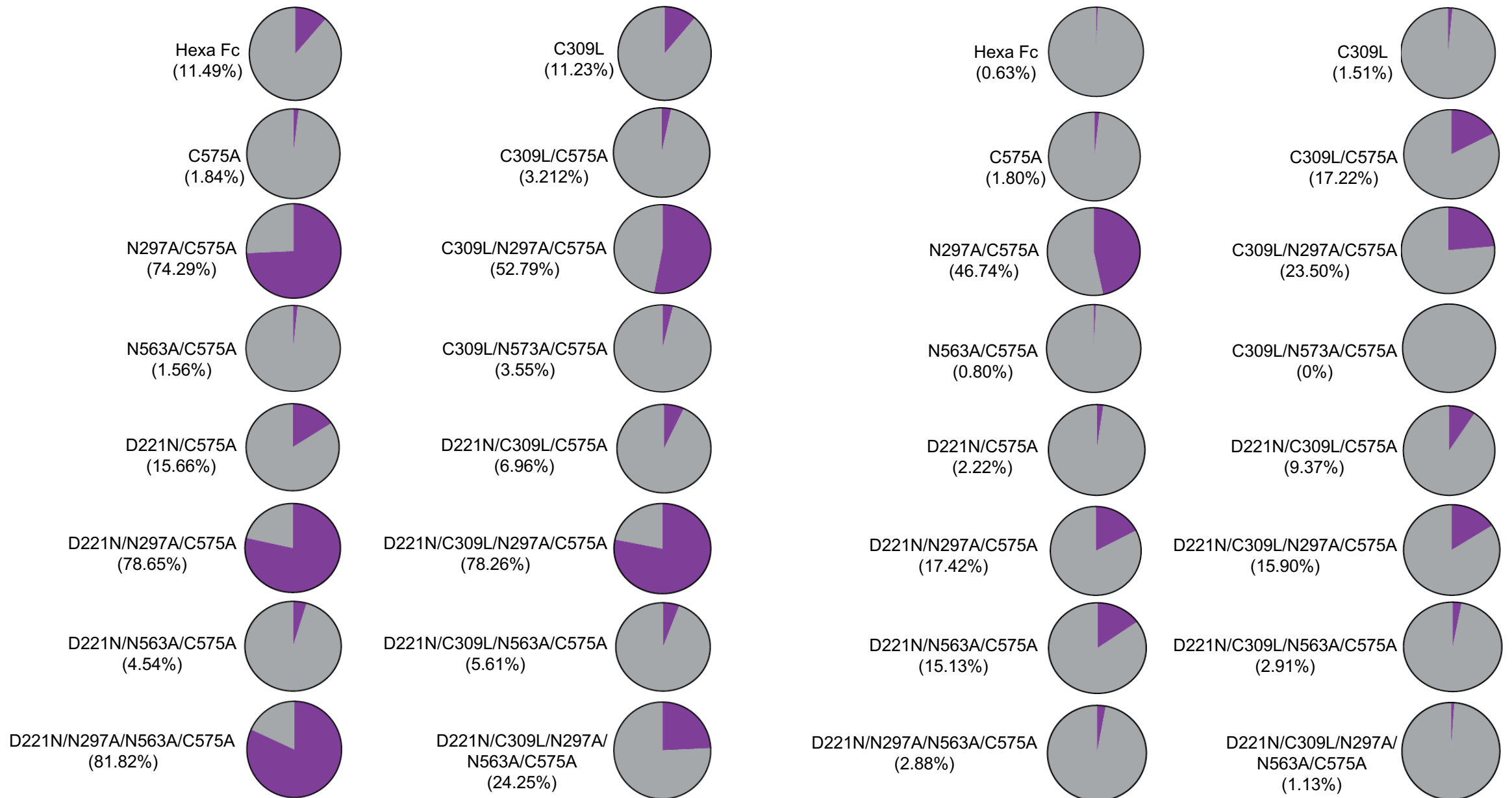


Fig. 11

